Controlling the absorption dynamic of water-based ink into porous pigmented coating structures to enhance print performance

Cathy J. Ridgway and Patrick A.C. Gane

Keywords: absorption, ink setting, digital printing, water-based inks, ink holdout, flexography, porous structures, coating structure for digital printing, digital paper coating, silica, calcium carbonate

SUMMARY: Previous work (*Gane, P.A.C. and Ridgway, C.J., Advances in Printing Science and Technology Volume 27, 2001*) has shown that the absorption of the fluid phase from a water-based flexographic ink is affected by the polymer content in the fluid phase, filtercake formation within the contacting ink layer and the distribution of dissolved polymer between the filtercake and the coating structure. The study showed that enhanced setting rate could be obtained by controlling the surface area to porosity ratio of the printing surface. This paper now reports the effect on absorption dynamic and ink component holdout of introducing two different materials, each with a different form of porosity-creating structure, as constituents of consolidated tablets. These are (i) a high surface area highly porous precipitated silica, which under compression generates a structure with fine pores, and (ii) a novel relatively high surface area deformable calcium carbonate structure consisting of porous spherical aggregates covered with small plate-like crystals which consequently create a high permeation tortuosity. Both the materials had a median particle size of approximately 1 µm and were studied both in combination with standard dispersed ground calcium carbonate as well as on their own. A porous network model, Pore-Cor, was used to exemplify the important structural features of the porous structure controlling the inertial and viscous fluid uptake dynamics which in combination act to make broad pore size distribution structures containing fine pores absorb faster than more monosize distributions consisting predominantly of either fine or large pores. The centrifuged fluid phase of a flexographic ink was used as representative of a complex polymer-containing water-based dye ink which could be considered for standard flexography or as might be encountered in digital ink jet printing. Residual pigment in the centrifuged fluid phase was shown to be excluded from all the structures tested. The dissolved dyes readily enter the silica interstitial structures but not the novel carbonate structures, illustrating the effect of using high adsorptive surface area acting together with extended wetting front residence time (low permeability) to aid retention of dyestuff at the surface of a coating. This indicates that the novel carbonate can be used in paper coatings to give an enhanced print colour density along with a reduction in ink demand.

ADDRESS OF AUTHORS: Omya AG, CH-4665 Oftringen, Switzerland.

Water-based digital and flexographic printing, with their use of environmentally friendly inks are increasing in importance especially for 'point of sale packaging' due to the requirement to create marketing appeal for cartons and boxes, and personalised products. The development of flexography over the years has been described by Moir (1994). High standards of print quality are nowadays expected and, because of this, coated grades of bleached board and unbleached Kraft liner are in increasing demand. For such printing using water-based flexographic inks, rapid drying characteristics are essential, and can be achieved through evaporative loss aided by additives which reduce surface energy and increase fluid phase partial pressure, and by providing strongly absorptive coating layers, which are of particular importance when considering multi-colour formats. The development of print-on-demand ink jet technologies is more recent and places similar demands on print surface structure design for both printing and writing papers as well as board. For increased resolution and print quality, coated grades often contain speciality pigments and formulations such as precipitated silica and polymer additives.

Such absorptive coating layers can be produced using the blocky particle morphology of ground calcium carbonate, generally of relatively fine particle size, as a basis and additional high surface area pigments are of benefit to enhance the capture of dyes and to promote controlled absorption of the fluid phase of the ink. To achieve coverage, multi-layer coating is often employed in which the precoat layers can have larger pore size and greater porosity than the subsequent fine topcoat. However, the rate of absorption is not controlled wholly by the absolute level of porosity: the distribution of pore sizes in the coating structure network is equally important especially when considering the rate of absorption. The importance of preferred pathway absorption has been described by Schoelkopf *et al.* (2000a). There is a need for the high capillarity developed in the finer pores in order to ensure rapid absorption during the short times in which the ink is in contact with the coating layer during high-speed printing processes to avoid blocking, i.e. marking of adjacent surfaces, feathering and bleeding. This high capillarity is required in particular to overcome the additional drag which is created by the partially viscosifying ink layer. Xiang and Bousfield (1998) proposed a model for the formation of an interface filtercake between the ink and the coating surface and its retardational drag effect. For optimal absorption properties it is necessary to consider the force balance between the capillary absorption into the network and the permeability characteristics of any retained pigments and polymers forming the filtercake rather than simply strive for ever greater porosity.

Previous work (Gane, Ridgway 2001) has shown that the absorption of the fluid phase from a flexographic ink is affected by the following: (a) the polymer content in the fluid phase of the ink, (b) filtercake formation within the contacting ink layer, which acts as a filter for the capture of dissolved polymer, (c) distribution of dissolved polymer between the filtercake and the coating structure which controls the rate of fluid absorption. There can also be a retardational effect due to solved polymers coating the pore surfaces of the network coating structure. An enhanced setting rate for a flexographic ink could be obtained by controlling the surface area to porosity ratio of the printing surface. It was therefore predicted that an enhanced setting rate of a flexographic ink could be obtained whilst maintaining some residual porosity within the immobilised ink structure. This polymer adsorption effect is equally applicable to ink jet inks which contain both surfactants and dyes.

The present paper studies the quantification of the effects experimentally and theoretically of introducing two different forms of increased coating porosity that can be generated by using (a) a high surface area porous precipitated silica[1] with a median pore diameter of 4 µm and an oil absorption volume of

[1] GASIL Silica 35M, Crosfild Limited, Warrington, England, WA5 1AB, UK.

200 g/100 g, which generates a structure with a multitude of fine pores, and (b) a novel high surface area compressible calcium carbonate structure used to introduce reduced permeability whilst retaining high adsorption power.

Experimental absorption rates are studied using a technique of fluid absorption into porous compressed pigment tablets (Schoelkopf *et al.* 2000b). This is effectively a wicking experiment.

A computer model, Pore-Cor[2], is used to simulate the permeation of the centrifuged fluid phase of a flexographic ink into the 100 % silica porous structures by applying a wetting algorithm for fluids undergoing both inertial and viscous dynamical absorption. Pore-Cor cannot model the potential clogging effects of dissolved polymer. Its use in the analysis is therefore limited to highlighting the principal important qualitative structural features of the structures. Understanding the features responsible for the absorption dynamic assists greatly in the design of suitable coatings for fluid ink applications.

The Pore-Cor model of porous structures

Pore-Cor is a computer model that simulates the void-space structure of porous materials. It has been used to simulate the structures of a wide range of porous materials including sandstones (Matthews *et al.* 1996), medicinal tablets (Ridgway *et al*. 1997) and soil (Peat *et al.* 2000). Pore-Cor uses a unit cell with 1 000 cubic pores in a three dimensional 10x10x10 array, connected by up to 3 000 throats, (i.e. one connected to each cube face), which in this work are assumed double conical (11), representing the realistic divergence and convergence of geometries associated with spherical and blocky pigment morphologies (Toivakka, Nyfors 2001). Each pore is equally spaced from its neighbouring pores by the 'pore row spacing' *Q*, and each unit cell is a cube of side length 10 *Q*. There are periodic boundary conditions, which are applied serially during wetting, with each cell connected to another identical unit cell in each direction. When used to simulate actual samples the pore- and throat-size distributions of the unit cell are optimised so that the simulated non-wetting percolation curve fits as closely as possible to the experimental mercury intrusion curve (Matthews *et al*. 1995), corrected for mercury compression, penetrometer expansion and sample compression (Gane *et al.* 1996). The distributions of pore and throat sizes are characterised by two parameters, 'throat skew' and 'truncated pore skew'. The throat skew is the percentage number of throats of the smallest size. The distribution of throat sizes is log-linear and pivots about its mid-point at 1 %. The truncated pore skew increases the sizes of the pores by a constant multiple. However, the pores whose sizes then become larger than the experimentally determined maximum are truncated back to the size of the largest throat, thus giving a peak in the distribution at the maximum size. The positions of the pores and throats within the defined matrix are random, determined by a pseudo-random number generator.

A matrix of values of throat skew and connectivity (the average number of throats per pore over the whole unit cell) are refined on a trial basis, and the void structure which has percolation characteristics most closely matching the experimental intrusion curve is selected (Matthews *et al.* 1995). The percolation characteristics of the network are insensitive to *Q*. Therefore, the *Q* value of the chosen structure is adjusted so that its porosity matches the experimental value while ensuring that no pores overlap. If the experimental porosity value cannot be simulated then the truncated pore skew parameter needs to be used, thus introducing larger pores and allowing greater porosity values to be modelled. It is not normally possible to represent the full true complexity of the void network of a natural sample using the relatively simple geometry of the Pore-Cor unit cell. One reason is that the size of the unit cell is often smaller than the representative elementary volume (REV) of the sample. Therefore, different unit cells must be generated using different seeds for the pseudo-random number generator. The algorithm is designed so that different structural parameters in conjunction with the same seed of the pseudo-random number generator produce a family of unit cells which are similar to each other; for example, all may have a selected group of large pores in the same region (Peat *et al*. 2000). Different stochastic generations use a different pseudo-random number generator seed, and can either use the original Pore-Cor optimisation parameters or can be re-optimised to the experimental data.

The wetting equations derived in a previous publication (Ridgway *et al*. 2001) were used to calculate the wetting flux in each pore and throat in the void network. It was assumed that inertial flow occurred when fluid began to enter each throat, initially wetting the throat in the form of a monolithic block of fluid (Schoelkopf *et al.* 2000a). The inertia of the fluid caused a retardation of wetting of the larger features, at short times after initial entry into a throat feature, relative to that predicted by the Washburn equation. Once a double-conical throat was completely full, the volumetric flow rate at the throat exit was calculated, and used to calculate the rate of fill of the adjacent adjoining pore. A pore could be filled by the fluid from more than one throat, which could start to flow into it at different times. Once a pore was full, it started to fill the throats connected to it that were not already full and which were not already filling from other pores. If at any stage the outflow of a pore exceeded the inflow, then a restriction due to conservation of mass was applied, which removed any imbalance and restricted the flow of fluid further into the network.

Materials and methods

Pigments - ground calcium carbonate, silica, novel calcium carbonate

Three pigments were used in these studies and a summary of their properties is given below in *Table 1.*

Silica has the highest surface area and smallest particle size distribution followed by the novel calcium carbonate and then the HC60[3] which has the broadest particle size distribution and the lowest surface area.

The novel calcium carbonate is derived from standard ground calcium carbonate and consists of a rose-like morphology of fine spherical porous aggregates, the surface of which is formed from smaller platelets, as shown in *Fig. 1.* The use of such a pigment as a filler for improved calenderability of supercalendered paper grades is discussed elsewhere (Blixt *et al*. 2001).

[2] Pore-Cor is a software program of the Environmental and Fluids Modelling Group, University of Plymouth, PL4 8AA U.K.

	HC60	Novel calcium carbonate	Silica
Surface area (BET) /m^2g^{-1}	6.5	62	262.4
% by weight less than			
< 10 µm	99		
< 5 µm	92	99	100
< 2 µm	60	82	91
< 1 µm	40	35	57
< 0.5 µm	23	18	24
< 0.2 µm	12	14	6
Median particle size (D50%) /µm	1.5	1.3	0.9
Top cut (D98%) /µm	10	5	3

Table 1. *Surface area and particle size distribution of pigments.*

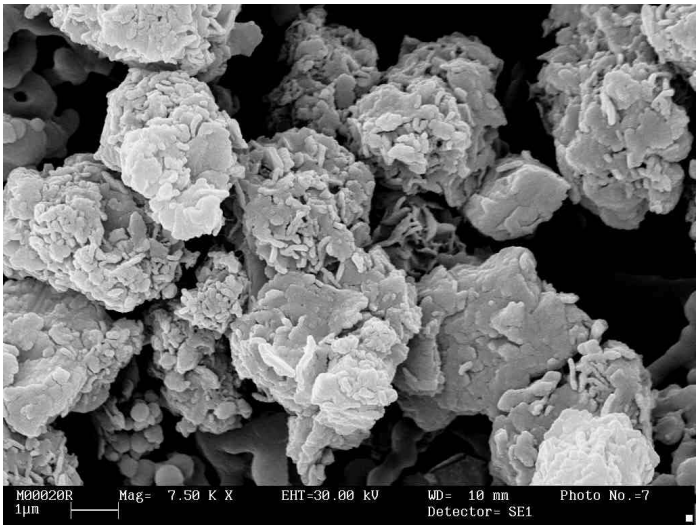

Fig. 1. Novel calcium carbonate used to make compressible tortuous tablets.

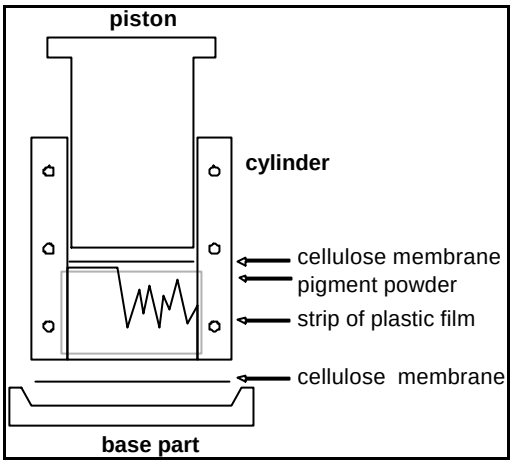

Fig. 2. Schematic cross-section of the die showing the plastic lining and cellulose membrane (Gane et al. 2000).

Making the tablets and blocks

Many valuable investigations can be performed directly on paper surfaces or on model coating layers. However, a paper coating has a thickness, depending on grade, of between 5-15 µm, and a practical single ink layer is typically 0.25 µm (or in total on a four colour press ~1 µm). It is to be expected that using even volumes as small as a micro litre directly onto such a microscopic surface volume is distinctly limited by saturation phenomena when it comes to understanding the complexities of coating imbibition. Because of these limitations, macroscopic blocks of consolidated pigment were formed over a range of compressions which allowed for the investigation in detail of capillary absorption and the relationship of initial pore filling to factors such as surface chemistry and geometry of the pigmented pore structure as a function of sample compression.

For the preparation of these pigment tablets a 4.5 cm internal diameter cylindrical hardened steel die attached to a baseplate with a single acting upper piston is used which is suitable for a wide range of pigment particle sizes, chemistries and morphologies. The die is divisible into two parts to aid removal of the compacted pigment sample and the walls of the die are protected with a strip of plastic film to prevent sticking of the powder to the wall and to reduce edge friction, *Fig. 2.*

A number of tablets were made using mixtures of a spray dried predispersed natural ground calcium carbonate derived from limestone (HC60)[3] with progressive additional amounts of silica and novel calcium carbonate. The weight ratios of additional high surface area pigment to HC60 were chosen to be 0:100, 5:95, 10:90 and 20:80. Samples were also made using 100 % of the high surface area pigments. The pigments were mixed using a mechanical stirrer, and then used to make tablets over a range of pressures. The pigment was compacted in the hydraulic press for 5 minutes at a predetermined pressure. The range of applied press forces F_p, the press area A_p, and the resulting pressures are listed in *Table 2*.

The tablets were cut and ground to form several 12 mm cubic blocks, using a rotary disc grinder and a specially constructed, precisely adjustable jig. To reduce artefacts caused by the wetting of their outer surfaces during the absorption experiments, samples were coated with a thin barrier line of silicone around the base of the vertical edges arising from the basal plane. The remainder of the outer planes were not coated to allow for the free movement of displaced air during liquid absorption and to minimise any interaction between the silicone and the absorbed liquid.

[3] HC60 is used to denote Hydrocarb 60, a product name of Omya AG, Baslerstrasse, CH 4665 Oftringen, Switzerland

Cross-sectional area, A_p = 17.35 cm^2 (±0.16)	
Applied force F_p / kN (±5)	Effective pressure $P=F_p/A_p$ / MPa (±2.7)
300	172.9
400	230.6
450	259.4

Table 2. *Conversion table of applied forces to resulting pressures experienced in the tablet press.*

Wetting apparatus

The rate of fluid uptake was measured using an automated microbalance, namely a PC-linked Mettler Toledo AT460 balance with a precision of 0.1 mg, capable of 2.7 measurements per second. To provide a sufficiently slow and precise approach of the sample down to the liquid surface, a special sample holder was constructed according to Gane *et al*. (2000), *Fig. 3.* The chamber around the balance base plate enabled a controlled atmosphere to be established, shielded from external air and humidity. There was a gas inlet, which could be used to keep the cell under a steady stream of an inert gas such as nitrogen.

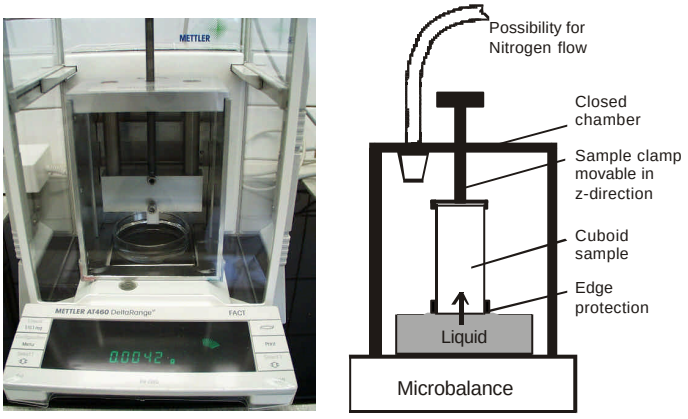

Fig. 3. Gravimetric wetting apparatus (Schoelkopf et al. 2001)

All apparatus, gases and samples in this study were maintained at 23.0 ±1.5°C. Prior to the absorption experiments, each porous block sample was placed in a 5 litre chamber. The chamber was then flushed through with dry nitrogen, and the sample left to equilibrate for 48 hours. The absorption experiments themselves were performed in the balance chamber described above, which was flushed with a steady stream of dry nitrogen flowing at 1 litre min^{-1}. The evaporation rates of the fluid phases from the supersource reservoir were measured with a dummy non-wetting, non-absorptive sample block in place of the experimental sample so the absorption data could be corrected for this apparent weight difference.

Using this technique the micro-scale absorption characteristics of structures could be scaled to observably realistic volumes under supersource conditions.

Mercury porosimetry

A Micromeritics Autopore III mercury porosimeter was used to measure the percolation characteristics of the samples. The maximum applied pressure of mercury was 414 MPa (60 000 psia), equivalent to a Laplace throat diameter of 0.004 µm. The equilibration time at each of the increasing applied pressures of mercury was set to 60 seconds. The mercury intrusion measurements were corrected using the software Pore-Comp [4] for the compression of mercury, expansion of the glass sample chamber or 'penetrometer' and compressibility of the solid phase of the sample which adopts the following equation from Gane *et al.* (1996):

$$V_{\text{int}} = V_{\text{obs}} - dV_{\text{blank}} + \left[0.175(V^1_{\text{bulk}})\log_{10}\left(1+\frac{P}{1820}\right)\right] - V^1_{\text{bulk}}(1-\Phi^1)\left(1-\exp\left[\frac{(P^1-P)}{M_{\text{ss}}}\right]\right) \quad \textbf{[1]}$$

V_{int} is the volume of intrusion into the sample, V_{obs} the intruded mercury volume reading, dV_{blank} the change in the blank run volume reading, V^1_{bulk} the sample bulk volume at atmospheric pressure, P the applied pressure, Φ^1 the porosity at atmospheric pressure, P^1 the atmospheric pressure and M_{ss} the bulk modulus of the solid sample. The volume of mercury intruded at the maximum pressure, once corrected for sample compression effects, can be used to calculate the porosity of the sample.

Characterisation of the centrifuged fluid phase of a flexographic ink

The absorption studies made in this work compare the complexity of a flexographic ink with that of water. Other water-based ink types will be expected to show similar qualitative effects. To make the study universally applicable, the fluid phase of the ink was studied separately.

The multi-phase system constituting a flexographic ink is separable into a liquid phase and a solids-containing structural phase. A sample of a typical flexographic ink[5] was centrifuged in a Sigma laboratory centrifuge 2-15[6] at 35 000 min^{-1} for 45 minutes. The top (supernatant) phase was syringed into a separate vessel and centrifuged again. This process was repeated four times. The resultant separated continuous phase was examined by a Mastersizer S[7]. It was shown to contain a residual small quantity of pigment particles with a size distribution shown in *Fig. 4.* We see that the particles of pigment are large relative to the fine pores expected in a paper or board coating and, as we see later, this results in exclusion of the pigment from the structures under study. The fluid also contained soluble red dye which was used as an adsorption tracer during the subsequent absorption experiments.

[4] Pore-Comp is a software program developed by the Environmental and Fluid Interactions Group, University of Plymouth, PL4 8AA, U.K.

[5] Rot VSW 230, a product of Printcolor Gravoflex AG, CH-4800 Zofingen, Switzerland.

[6] Merck eurolab, Merck KGaA Darmstadt, Germany.

[7] Malvern Instruments Ltd., Malvern, UK.

Density / kgm^{-3}	Viscosity / $kgm^{-1}s^{-1}$	Surface tension / Nm^{-1}	Contact angle for fluid on dispersed calcite / ^{o}	Polymer concentration / %
1 035	0.0113	0.0338	16.65	26.27

Table 3. *Properties of centrifuged fluid phase from flexographic ink.*

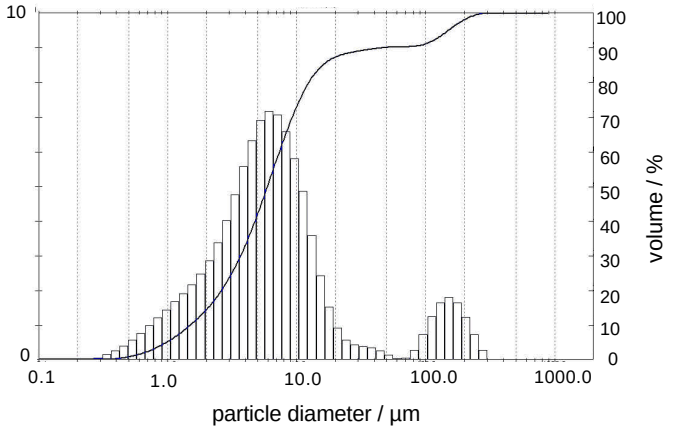

Fig. 4. Particle size distribution in centrifuged ink fluid phase.

The fluid phase obtained by centrifugation has also been shown to contain film forming polymers (Gane, Ridgway 2001). FTIR spectra which were run over a wave-number range from 400 to 4 000 cm^{-1} in transmission mode using a silver chloride carrier showed characteristic absorptions for such substances as styreneacrylate and resin. There were also absorptions indicating alkyl ketone dimers together with some bands in the centrifuged fluid phase due to incomplete removal of what was assumed to be organic pigment. Other absorptions were assignable to a range of compounds including glycols, esters, alcohols, fatty acids and salts.

The viscosity of the centrifuged fluid phase was shown to be a constant at constant shear stress independently of time. Any rheological effect arising from dissolved polymer was therefore assumed to be small at least at the initiation of concentration, i.e. at the starting solution concentration, and a characteristic viscosity was therefore assumed.

Further measurements were made of the density, surface tension, contact angle and polymer content, the results of which are shown in *Table 3* and the methods used to obtain the values are described in a previous publication (Gane, Ridgway 2001).

Results and discussion

Mercury intrusion

100 % silica and 100 % novel calcium carbonate tablets

The mercury intrusion curves, after the Pore-Comp corrections had been performed, are shown in *Fig.* 5.

The intrusion curves for the silica tablets showed a decrease in intrudable volume as the pressure used for making the tablets was increased. The porosity for the samples compressed at 300 kN, 400 kN and 450 kN are 58 %, 53 % and 50 %, respectively, showing the tablets are becoming more dense at higher pressures. The 50 % intrusion diameters, d_{50}, are 0.008 µm, 0.007 µm and 0.007 µm for the 300 kN, 400 kN and 450 kN compacted tablets, respectively, showing there is little change in the actual median void size despite the reduction in porosity. The pore size distributions are fairly monosize and the effect of increased pressure is to introduce some finer pores which play an important role in the absorption dynamic together with effective closure of some parts of the structure. This is in contrast to previous studies looking at a broad size distribution pharmaceutical grade crystalline lactose and an anti-inflammatory compound powder compression where increased pressure on the tablet resulted in a reduced d_{50} value (Ridgway *et al*. 1997). *Fig.* 6 shows the structure for a 100 % silica tablet compressed to 300 kN. The narrow size distribution is clearly seen.

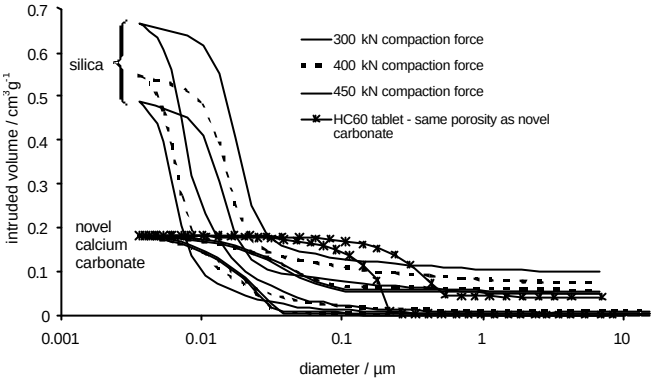

Fig. 5. Intrusion curves for 100 % silica and 100 % novel calcium carbonate tablets

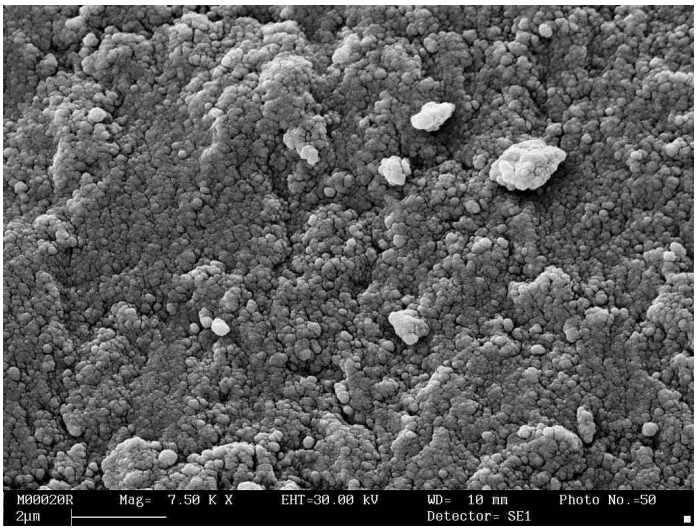

Fig. 6. Electron micrograph of silica taken from a tablet compressed to 300 kN.

On the other hand, the intrusion curves for the novel calcium carbonate tablets show the same volume of intrusion for all three compaction forces, (the novel calcium carbonate intrusion curves overlie one another in *Fig. 5*). It is known that the structure is deformed during the calendering process of paper making where a pressure of up to 50 MPa is applied. Pressures far in excess of this value are applied when the tablets are made and therefore the outer layer of the spherical aggregates are deformed or squashed. *Fig. 7a* and *Fig. 7b* show the novel calcium carbonate structures after compaction forces of 300 kN and 450 kN, respectively. The surface

aggregates are no longer apparent. The extent to which the structure is compressed cannot, therefore, be clearly determined using mercury porosimetry, and as specific surface area of the tablets themselves were not determined it is not possible to specify the effect on potential adsorption. Further compression of the tablets does not result in any further porosity reduction. The intrusion data show a d_{50} of 0.018 µm, and a porosity of 33 % for all the tablets. These porosity values were verified by known oil mass absorption (at saturation) and also by actual volume and density measurements.

a)

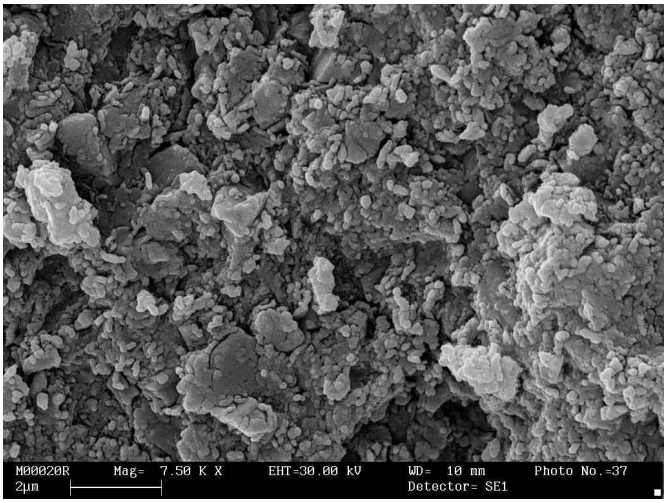

b)

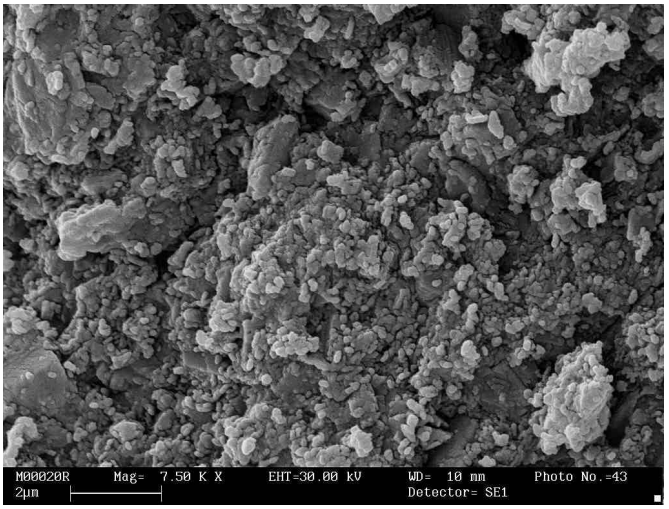

Fig. 7a and Fig. 7b. Electron micrographs of novel calcium carbonate taken from a tablet compressed to a) 300 kN and b) 450 kN.

Also shown in *Fig. 5* is the mercury intrusion curve for a compressed tablet of HC60 where the resulting porosity was 33 %, the same as that for the novel calcium carbonate tablets. The d_{50} value is clearly larger with a value of 0.18 µm. An electron micrograph of an HC60 tablet compressed to 100 kN is shown in *Fig. 8.* The broad void size distribution is clearly distinguishable when this picture is compared with that of the silica in *Fig. 6.*

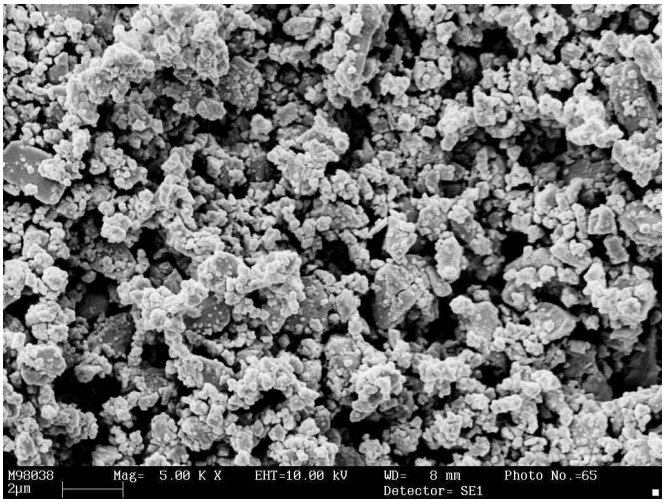

Fig. 8. Electron micrograph of HC60 taken from a tablet compressed to 100 kN.

Silica or novel calcium carbonate mixed with HC60

A range of porosities was achieved for each ratio of additional high surface area pigment to HC60 by changing the compression pressure, *Fig. 9.* The addition of the high surface area pigments caused an increase in the porosity which was more pronounced for silica than for the novel calcium carbonate. It is clear that with different additions of the novel calcium carbonate the same porosity could be achieved over a significant range of applied pressures indicating the conformable nature of the material. This gives the opportunity for strongly adjusting the experimental surface area to porous volume ratio by increasing the amount of the novel calcium carbonate additive. Conversely, in the case of the silica, the surface area to porosity ratio follows more linearly with amount of silica used.

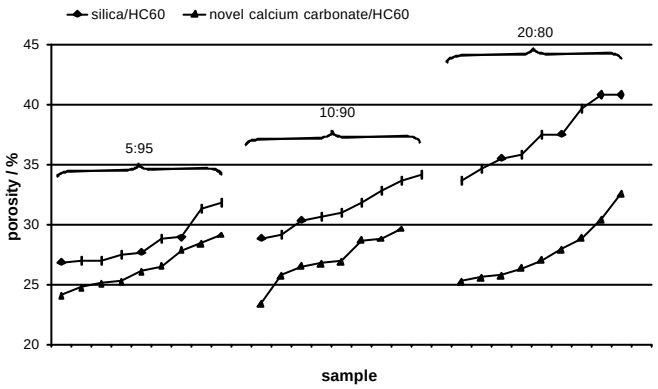

Fig. 9. Porosities of HC60/high surface area pigment mixes.

The mercury intrusion curves for these samples were corrected as previously described for mercury compression and penetrometer expansion using the program Pore-Comp. Four samples over the mix range for each additional pigment were selected with the aim of isolating the porosity effects and also isolating the effects introduced by the addition of the high surface area pigment. This was achieved by selecting two samples for the 5 % addition level which had different porosities, one sample from the 10 % addition level which had the same porosity as the more porous of the 5 % samples, and finally one at 20 % addition which had yet higher porosity.

The mercury intrusion curves give an indication of the internal void structure of the tablets. These are shown below,

in *Fig. 10* and *Fig. 11* respectively, for the novel calcium carbonate and the silica mix tablets.

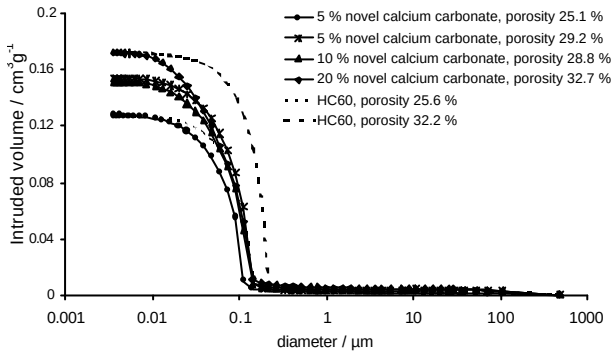

Fig. 10. Mercury intrusion curves for HC60/novel calcium carbonate samples.

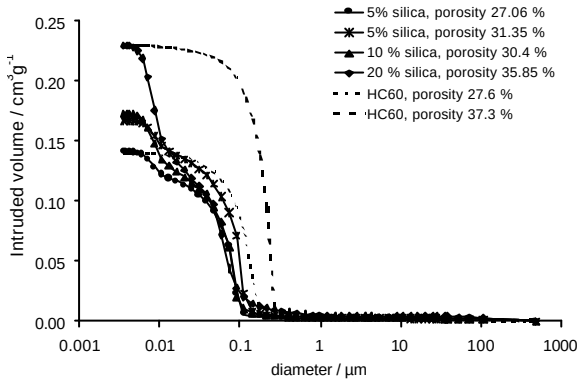

Fig. 11. Mercury intrusion curves for HC60/silica samples.

Fig. 10 and *Fig. 11* additionally show the intrusion curves for two 100 % HC60 tablets of porosity equal to the highest and lowest values of the respective mixed tablets. The mercury intrusion curves for the HC60/novel calcium carbonate tablets show that the pore sizes are reduced once the new pigment is introduced as the mercury intrusion occurs at a higher pressure. The permeability of the structures will be reduced due to the smaller pore sizes. The surface area will therefore have been increased for the HC60/novel calcium carbonate tablet, which has a more closed structure, when compared with a tablet of the same porosity made purely of HC60. The novel calcium carbonate has filled the larger pores and added pores similar to the smaller sizes resulting in a smaller mono modal size distribution.

The HC60/novel calcium carbonate structures have a d_{50} of approximately 0.1µm. In contrast, the HC60 mercury intrusion curves have a steeper gradient and show a larger d_{50} value than the equivalent HC60/novel calcium carbonate structures.

Adding silica to HC60 increases the porosity much more than the addition of novel calcium carbonate, *Fig. 11.* The pore sizes are reduced as before and there is a much greater increase in the number of finer pores as indicated by a step in the intrusion curves at a diameter of 0.01 µm. The size of the step correlates directly with the amount of silica added. The silica is again filling in the original larger pores of the HC60 structural packing but also adding smaller pores. There is likely to be an increase in the permeability due to the large increase in porosity, and also an increase in surface area which gets greater the more silica is added. These structures are more open than the equivalent HC60 structures and have a bi-modal void size distribution.

Absorption of fluids - the role of polymer as an absorption retardant

The absorption dynamics of water versus the centrifuged fluid phase of the flexographic ink were studied to establish the action of dissolved polymer in the fluid phase. Depending on the absorption rate, pore size distribution and absolute level of concentration, the deposition, adsorption or precipitation of polymer can occur either within a forming interface filtercake or within the porous absorbing structure or both. For example, the effect of surfactant on the absorption rate of water into a porous structure is well documented and is retarded compared with simple wetting fluids due to the dependence of the wetting front progress on the diffusion of the polymer and its adsorption-desorption rate onto the side walls of the porous medium. Furthermore, size exclusion of polymer from the porous structure would lead to blanking off of entry pores effecting a further contribution to drag. This extra drag contribution is clearly shown in *Fig. 12* where the experimental absorption dynamic for the centrifuged fluid phase is compared with that of pure water as they are absorbed into a 100 % silica porous structure. The absorption is expressed as the mass of fluid absorbed per unit area of the external sample surface contacting the fluid reservoir.

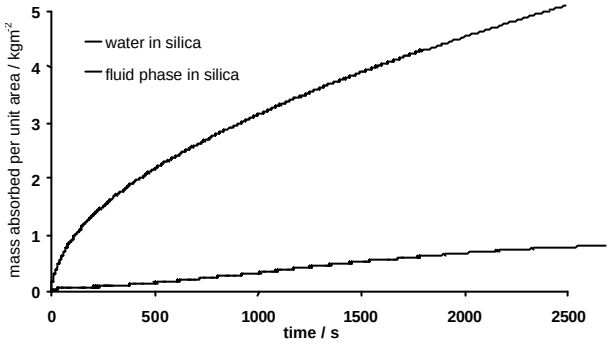

Fig. 12 Absorption into a 100 % silica porous block comparing the ink fluid phase with pure water.

The absorption curves have been corrected for both the effect of evaporation and for the initial wetting jump that occurs when the tablet sample is first lowered into the fluid using the method of Schoelkopf *et al.* (2000b). The equations for the wetting jump correction are shown in the *Appendix.*

The absorption curves for the ink fluid phase into the previously chosen 100 % silica and 100 % novel calcium carbonate structures are shown in *Fig. 13*. The absorption curves are truncated at the point where the evaporation rate of the fluid phase is equal to that of the absorption of the fluid phase. The absorption of centrifuged fluid phase into a 100 % HC60 tablet is also shown for comparison.

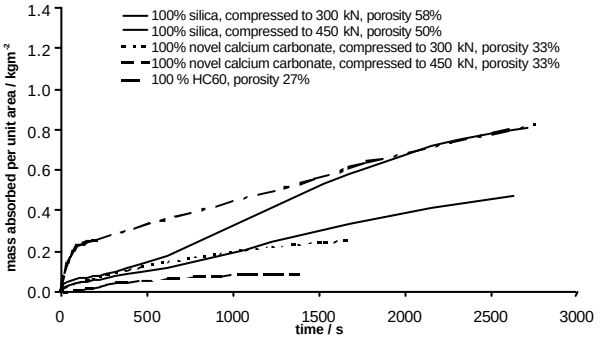

Fig. 13. Absorption curves for 100 % silica and 100 % novel calcium carbonate consolidated tablets compared at different formation compressions and with 100 % HC60.

The absorption curve for the HC60 tablet has a much steeper initial rise; this is due to the broader size distribution within the tablet (see *Table 1*). The effect of broadening a size distribution on the absorption behaviour was shown theoretically with the network model Pore-Cor by Ridgway and Gane (2001). The large voids act as reservoirs feeding the smaller voids which fill faster at the short time scales. The curve also has a point where the rate reduces which is where the polymer starts to seal the void structure due to size exclusion and evaporation at the wetting front outer surface.

The initial gradient of the absorption curves for the 100 % high surface area pigment structures are much lower. The novel calcium carbonate has an extremely narrow size distribution, as can be seen from *Fig. 7* (SEM) where the aggregates have almost identical sizes and, as shown by the steepness of the mercury intrusion curves, so have the pores. It is already known from other work (Ridgway, Gane 2001) that a narrow size distribution leads to an initial low absorption rate. The difference between the two novel calcium carbonate curves is thought to be due to the deformation of the structure of the pigment during the tablet compression, however, as discussed previously, the exact changes in the pore structure are not known precisely as the high pressure intruding mercury acts further to compress the deformable structure rendering differentiation difficult.

The absorption curves for the silica tablets lie above those for the novel calcium carbonate. The lower porosity of the two silica tablets has the faster absorption. The absorption rates for the silica follow the pattern expected from earlier modelling work (Ridgway, Gane 2001) with the block made at higher pressure, and consequently having the lower porosity, giving the higher absorption rate due to the promotion of preferred pathway wetting in combination with a broadening of the pore size distribution with a small increase in the number of the finest pores. A model of polymer uptake has previously been proposed by the authors, Gane and Ridgway (2001), which would suggest that the silica tablet may become more clogged.

Colouration of tablets after absorption measurements

As well as studying absorption rate, the distribution of colouration was also observed.

The only red colouration in the case of the 100 % novel calcium carbonate, seen after the absorption, was at the surface interface of the tablet. In contrast, the red dye was seen to have penetrated into the silica blocks. The broad size distribution HC60 also showed colouration within the sample reducing in intensity toward the wetting front. These effects are shown in the schematic in *Fig. 14.*

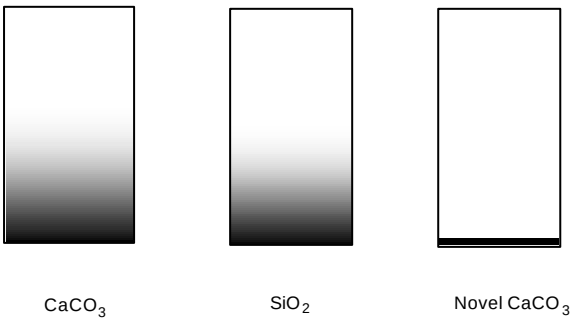

Fig. 14. Colour in blocks after the absorption experiment.

The exclusion of the red dye dissolved in the fluid phase from the novel calcium carbonate samples can be ascribed to the very high surface area of the novel calcium carbonate combined with its low permeability providing a greater capability for adsorption whereby the dye is held at the surface of the block while the remaining fluid continues to be absorbed. This effect is similar to that seen by Rousu *et al.* (2001) in the case of the chromatographic separation of offset ink fluid components which was seen to be increased as a function of pigment surface area and residence time at the wetting front (high surface area, low permeability gives maximum chromatographic separation). Subsidiary experiments have confirmed this where aqueous dye solution (Nickel (II) phthalocyanine-tetrasulphonic acid[8], 0.24 % solid content) placed on the surface of a silica block penetrated rapidly to a depth of 2 mm as observed by sectioning the block, whereas on the surface of a novel calcium carbonate block aqueous dye solution was adsorbed and the colour remained on the surface as a more intense hue.

The redness of the surface of the base of the tablets was measured using a Datacolor International Elrepho 3000 series. The instrument reports the colour in the form of the CIE colour standard. Measurements of *a* (extending from green to red), *b* (extending from blue to yellow) and *L** (the brightness) are given. The results are shown in *Table 4* below and *Fig. 15* shows the relevant quartile of a cross section of the CIELAB model. These results show that the novel calcium carbonate structures give values that lie closer to the red axis (lower *b* values) than the silica tablets which appear to have a higher yellow colour content. The colour hue between the pairs of tablets is consistent and the silica tablets have a higher hue than the novel calcium carbonate tablets.

[8] A product from Fluka Chemika AG, CH-9470 Buchs, Switzerland.

	Novel calcium carbonate	Novel calcium carbonate	silica	silica
Compaction force / kN	**300**	**450**	**300**	**450**
L*	71.08	74.28	69.25	71.25
a	43.06	39.16	41.65	34.95
b	25.64	20.14	37.03	32.23

Table 4 CIE analysis results for 100% silica and 100% novel calcium carbonate tablets after the absorption of the centrifuged fluid phase.

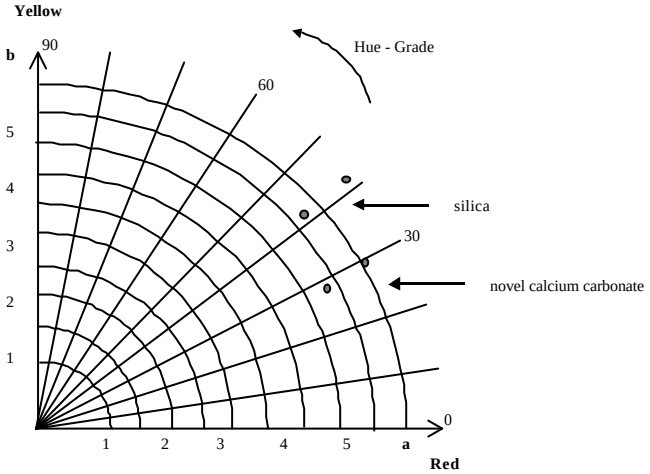

Fig. 15. CIELAB model showing colour measurement of silica and novel calcium carbonate tablets.

The adsorption of the dyestuff in the surface structure of the novel calcium carbonate structure acts to enhance the print colour density and is considered as a way to reduce the ink demand of coatings.

Inspection of the mixed sample blocks including silica showed that the colouration from the fluid phase was speckled as a result of the suspected heterogeneity of the mixture between HC60 and the silica, as shown experimentally in *Fig. 16* (5:95 silica to calcium carbonate). This illustrates very clearly the presence of an absorption competition. The speckled areas that were lighter in colouration indicated that the solved dyestuff enters less into, or is less adsorbed onto, the pigment which is rich in that area.

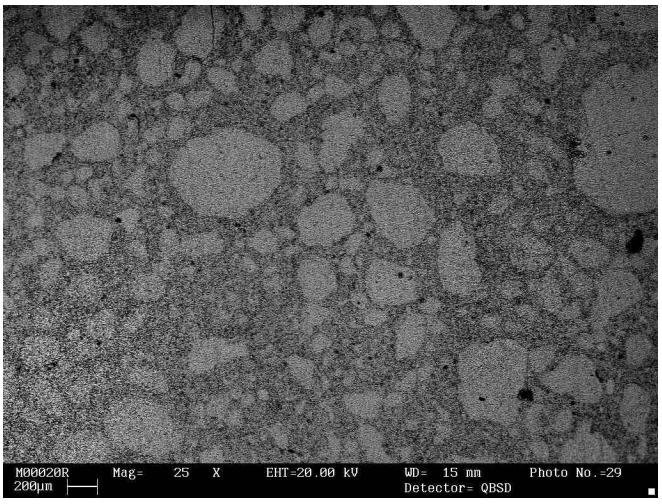

Fig. 16. Inhomogeneous dye adsorption in a tablet made from a blend of HC60 and silica.

Analysis of the elemental inhomogeneity was made using energy dispersive X rays (EDX). This is a micro analytical technique that is based on the characteristic X-ray peaks that are generated when the high energy beam of an electron microscope interacts with the specimen. Each element yields a characteristic spectral fingerprint that may be used to identify the presence of that element within the sample. The relative intensities of the spectral peaks may be used to determine the relative concentrations of each element in the specimen. The X-ray signal is detected by an energy dispersive solid-state silicon-lithium detector and the construction and efficiency of this detector sets a lower limit on the atomic number that may be detected. Using EDX-Analysis the element content of the sample in *Fig. 16* is shown in *Table 5*.

Elements	**Mass %**	**Atomic %**
Bright spot: Si	2.4	3.4
Ca	97.6	96.6
Dark spot: Si	15.2	20.3
Ca	84.8	79.7
Compounds		
Bright spot: SiO_2	2.1	
$CaCO_3$	97.9	
Dark spot: SiO_2	13.3	
$CaCO_3$	86.7	

Table 5. *Element content of HC60/silica mix tablet shown in Fig. 16*

The dye absorption/adsorption is less in the case of the standard carbonate-rich areas compared with the areas of high surface porous silica. The void sizes in the silica-rich areas are smaller than in the standard calcium carbonate areas and so the absorbed and/or adsorbed colour will also appear more intense in the silica-rich regions.

Absorption characteristics of complete ink

The 100 % high surface area pigment blocks of both silica and novel calcium carbonate showed no measurable absorption when the whole ink was used. This is assumed, after investigation, to be due to the colour pigment particles and polymers blocking the surface pores of the tablet block and resulting in an impermeable rapidly solidifying layer as the initial rapid surface wetting occurs causing virtually instantaneous drainage of fluid from the ink at the point of contact.

In contrast, however, the ink fluid penetrated readily into the mixed blocks and once again the mottled effect was clearly visible in the case of the HC60/silica mix indicating again the competitive adsorption of the dye and/or competitive absorption of the fluid.

	Minimum diameter / µm	Maximum diameter / µm	Throat skew	Truncated pore skew	Connectivity	Porosity / %	Unit cell size / µm
300 kN	0.0036	0.0309	0.96	1.3	2.9	58.4	0.319
450 kN	0.0036	0.0309	1.27	1.3	2.9	50.3	0.324

Table 6. *Pore-Cor parameters for 100 % silica tablets.*

Modelling the absorption of 100 % silica tablets

The fully corrected experimental mercury intrusion curves provide the percolation characteristics necessary for the generation of the model void structures using Pore-Cor. The Pore-Cor structures were determined for the 450 kN and 300 kN compaction force 100 % silica tablets and the absorption of the centrifuged fluid phase into these structures was simulated to illustrate the structural features associated with absorption dynamic. As mentioned previously, the Pore-Cor simulation cannot model the longer-time polymer absorption effects in terms of clogging, however the fluid properties of the actual fluid phase are used and Pore-Cor highlights the important qualitative structural features. Furthermore, the longer time scale absorption is not relevant for Pore-Cor due to the limited volumes provided by the single unit cell, and it is assumed that the polymer clogging effect occurs after longer time scale absorption. The corresponding size distribution of pores and throats for the Pore-Cor structure for the most compact silica tablet are shown in *Fig. 17*. It was necessary to use a truncated pore skew of 1.3 to match the experimental porosity. This truncated pore skew generated a peak in the distribution at the maximum experimentally observed pore size which is used as the truncation point of the pore size distribution.

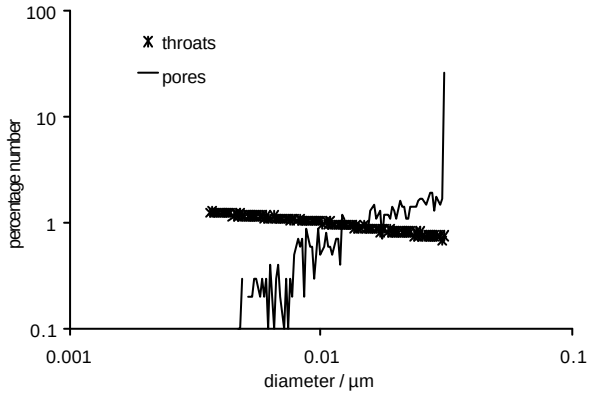

Fig. 17. Pore and throat size distribution for the 450 kN compaction force 100 % silica tablet.

Table 6 summarises the optimum Pore-Cor parameters for the two comparative samples and *Fig. 18* shows the simulated structure for the same sample as determined by the pore- and throat-size distribution illustrated in *Fig. 17*.

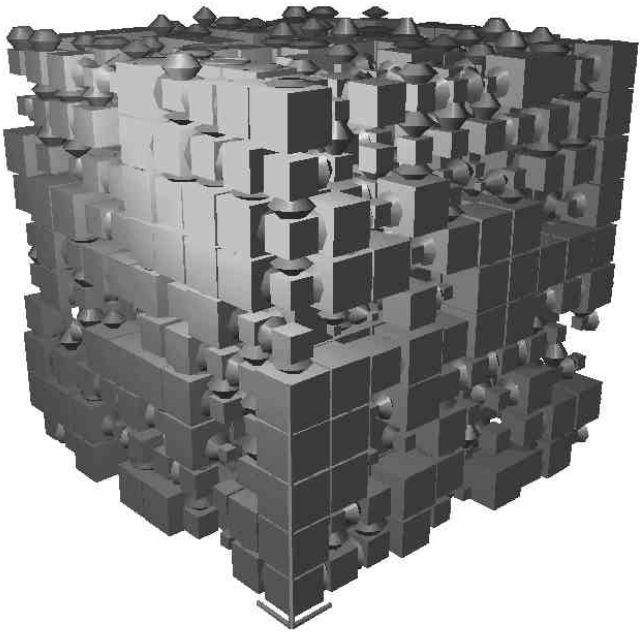

Fig. 18. Pore-Cor unit cell for silica compressed to 450 kN.

Fig. 19 shows the simulated wetting of the samples expressed as mass per unit area as a function of time for the centrifuged fluid phase using the properties shown in *Table 2.*

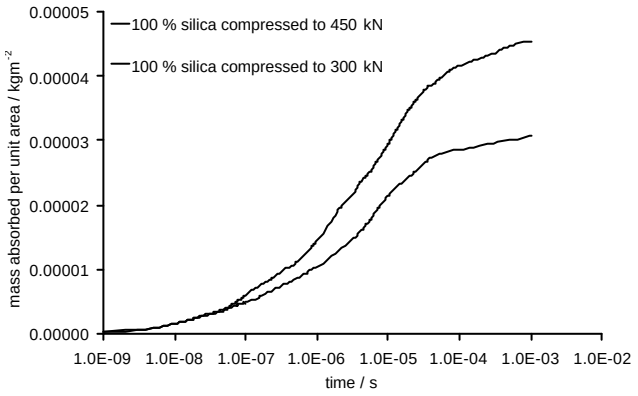

Fig. 19. Simulated absorption into 100 % silica tablets

The absorption rate into the more highly compacted tablet (450 kN) is greater than that into the less compacted tablet (300 kN), reproducing the observed order of the experimental results already seen in *Fig. 13.* Despite the short time scale used in the modelling, and hence the lower absorbed volumes compared with experiment, it is seen that the relative quantitative differences between the silica samples under the two compressions follows those seen in the practical experiment, *Fig. 13*.

The correlation between modelling and experiment permits us to demonstrate the importance of including inertial retardation and inertial wetting within our understanding of absorption into a porous network. Omission of these dynamical effects results simply in a reverse of the modelled

absorption dynamic between the more highly compressed and less compressed samples which would be contrary to experimental observation.

The use in the model of a pure fluid without polymer content, with the same viscous and surface tension properties as the experimental ink fluid, illustrates that the role of polymer adsorption, if leading to clogging, is minor when considering the relative differentiation in absorption rate between the different experimental structures, but, as shown by Ridgway and Gane (2001), can determine overall absorption rate and can be assumed to occur for structures having pore size distributions similar to these experimental samples despite very different surface chemistry, e.g. silica versus dispersed calcium carbonate. This statement of course ignores the effect of polymer clogging in a real ink filtercake and concentrates only on the effect in the porous structure. Therefore, clogging, if occurring, can be assumed to be a sample surface or near surface phenomenon controlling the delivery of fluid to the body of the structure.

The necessary distribution of pore sizes and pore shape, considered here in the model by using the double-conical throat construction for structures made from low aspect ratio particles, to develop a certain absorption dynamic for controlled ink fluid imbibition, can therefore be initially pre-determined. The model predicts that in the case of the experimental fluids applied in this work, the inclusion of fine pores into a structure with an inherent broad size distribution of pores increases absorption rate (throat skew 1.27 versus 0.96 simultaneous with reduced porosity - *Table 6*). Complementing this with reduced permeability, experimentally shown by the addition of the novel calcium carbonate, then increases the potential for ink holdout and, if supplemented by high dye adsorptive power, a high print density.

Conclusions

The network model Pore-Cor has been used to illustrate the structural features responsible for the differences in absorption rates between the unhindered wetting absorption of silica tablets formed at two different compaction forces based on inertial and viscous considerations. These results help to explain the absorption dynamic seen for a range of experimental pore size distribution based on addition of high surface area additive. It is shown that the need for optimised control of the setting characteristics of water-based inks cannot be met realistically by increasing the absorption rate to the point at which the ink immobilises instantly as this prevents ink levelling and leads to uneven pickup. Therefore the structure of the coating should be of high porosity but with a well-controlled absorption dynamic and permeability.

Homogeneous blends of high surface area porous pigments and standard ground calcium carbonate pigment are shown experimentally to provide the necessary control parameters for optimisation. The coating structure should contain a proportion of fine pores to provide sufficient capillarity. Advantageously, these fine pores should also have the ability to adsorb or capture dyestuff so as to enhance the print colour density. An example of a novel speciality calcium carbonate structure is used to create this effect by controlling the absorption rate into a structure of high surface area but low permeability. The novel calcium carbonate provides sufficient residence time during absorption to promote adsorption of the dye colour and therefore gives potential for higher print density. Low permeability in combination with high adsorptive power gives the possibility of retaining ink solids and dyes at the coating surface, thus increasing ink holdout and print density with the consequent benefit of reducing ink demand and increasing resolution.

Literature

Blixt, T., Balzereit, B., Laufmann, M. (2001): "A New Calcium Carbonate Concept for SC Papers", Proceedings of the CPPA, Montreal, Canada.

Gane, P.A.C., Kettle, J.P., Matthews, G.P., Ridgway, C.J. (1996): "Void Space Structure of Compressible Polymer Spheres and Consolidated Calcium Carbonate Paper-Coating Formulations", Industrial and Engineering Chemistry Research, *35*, 1753.

Gane, P.A.C., Ridgway, C.J. (2001): "Absorption Rate Studies of Flexographic Ink into Porous Structures: Relation to Dynamic Polymer Entrapment During Preferred Pathway Imbibition", Advances in Printing Science and Technology Volume 27, 56.

Gane, P.A.C., Schoelkopf, J., Spielmann, D.C., Matthews, G.P., Ridgway, C.J. (2000): "Observing Fluid Transport into Porous Coating Structures: Some Novel Findings", Tappi Journal, *85* , 1.

Matthews, G.P., Ridgway, C.J., Small, J.S. (1996): "Modelling of Simulated Clay Precipitation Within Reservoir Sandstones", Marine and Petroleum Geology, *13*, 581.

Matthews, G.P., Ridgway, C.J., Spearing, M.C. (1995): "Void Space Modeling of Mercury Intrusion Hysteresis in Sandstone, Paper Coating, and Other Porous Media", Journal of Colloid and Interface Science, *171*, 8.

Moir, W.W. (1994): "Flexography - a Review", JOCCA-Surface Coatings International, *77*, 221.

Peat, D.M.W., Matthews, G.P., Worsfold, P.J., Jarvis, S.C. (2000): "Simulation of Water Retention and Hydraulic Conductivity in Soil Using a Three-Dimensional Network", European Journal of Soil Science, *51*, 65.

Ridgway, C.J., Gane, P.A.C. (2001): "Dynamic Absorption into Simulated Porous Structures", TRI/Princeton International Workshop, Princeton,

Ridgway, C.J., Ridgway, K., Matthews, G.P. (1997): "Modelling of the Void Space of Tablets Compacted Over a Range of Pressures", Journal of Pharmacy and Pharmacology, *49*, 377.

Ridgway, C.J., Schoelkopf, J., Matthews, G.P., Gane, P.A.C., James, P.W. (2001): "The Effects of Void Geometry and Contact Angle on the Absorption of Liquids into Porous Calcium Carbonate Structures", Journal of Colloid and Interface Science, *submitted*,

Rousu, S.M., Gane, P.A.C., Eklund, D.E. (2001): "Influence of Coating Pigment Chemistry and Morphology on the Chromatographic Separation of Offset Ink Constituents", Twelfth Fundamental Research Symposium, Oxford 2001.

Schoelkopf, J., Gane, P.A.C., Ridgway, C.J., Matthews, G.P. (2000a): "Influence of Inertia on Liquid Absorption into Paper Coating Structures", Nordic Pulp and Paper Research Journal, *15*, 422.

Schoelkopf,J., Gane,P.A.C., Ridgway,C.J., Spielmann,D.C., Matthews,G.P. (2001): "Rate of Vehicle Removal From Offset Inks: a Gravimetric Determination of the Imbibition Behaviour of Pigmented Coating Structures", Tappi Fundamentals, San Diego,Tappi Press, Atlanta.

Schoelkopf, J., Ridgway, C.J., Gane, P.A.C., Matthews, G.P., Spielmann, D.C. (2000b): "Measurement and Network Modelling of Liquid Permeation into Compacted Mineral Blocks", Journal of Colloid and Interface Science, *227*, 119.

Toivakka, M., Nyfors, K. (2001): "Pore Space Characterization of Coating Layers", Tappi Journal, *84*, 49.

Xiang, Y., Bousfield, D.W. (1998): "The Influence of Coating Structure on Ink Tack Development", PanPacific and International Printing and Graphic Arts Conference,CPPA, Canada, 93-101.

Appendix

Smoothing correction equations used for the correction of the apparent initial weight change with time during the absorption of different fluids, according to Schoelkopf, Ridgway *et al.* (Schoelkopf *et al.* 2000b), where m is the corrected mass absorbed (g), t the time (s), a, b, c and d are fitting constants and R^2 is the standard measure of goodness of fit. The equation types shown are the simplest in each case which satisfy the criterion $R^2 > 0.98$.

100 % silica at a compaction force of 300 kN

$$m = a + bt^{2.5} + ct^3 + d\ln t$$

a = 48.033072, b = -0.000000871, c = 0.000000077,
d = -0.003335622, R^2 = 0.9945

100 % silica at a compaction force of 450 kN

$$m^2 = a + bt^{0.5}\ln t$$

a = 2275.736, b = -0.05529, R^2 = 0.9995

100 % novel calcium carbonate at a compaction force of 300 kN

$$m^2 = a + bt^{0.5}\ln t$$

a = 2235.49, b = -0.0556, R^2 = 0.9993

100 % novel calcium carbonate at a compaction force of 450 kN

$$m = a + bt\ln t + ct^{2.5}$$

a = 47.91326, b = -0.0000496, c = 0.0000000474, R^2 = 0.98